An insight into the mechanisms of nanoceria toxicity in aquatic photosynthetic organisms

Ismael Rodea-Palomares, Soledad Gonzalo, Javier Santiago-Morales, Francisco Leganés, Eloy García-Calvo, Roberto Rosal, Francisca Fernández-Piñas. An insight into the mechanisms of nanoceria toxicity in aquatic photosynthetic organisms. Aquatic Toxicology, 122–123, 2012, 133-143, https://doi.org/10.1016/j.aquatox.2012.06.005.

An insight into the mechanisms of nanoceria toxicity in aquatic photosynthetic organisms

Ismael Rodea-Palomares[1], Soledad Gonzalo[2], Javier Santiago-Morales[2], Francisco Leganés[1], Eloy García-Calvo[2,3], Roberto Rosal[2], Francisca Fernández-Piñas[1,*]

Ismael Rodea-Palomares[1], Francisco Leganés[1], Roberto Rosal[2], Francisca Fernández-Piñas[1,*]

[1] Departamento de Biología, Facultad de Ciencias, Universidad Autónoma de Madrid, Cantoblanco, E-28049 Madrid, Spain
[2] Departamento de Ingeniería Química, Universidad de Alcalá, Alcalá de Henares, E-28871 Madrid, Spain
[3] Advanced Study Institute of Madrid, IMDEA-Agua, Parque Científico Tecnológico, E-28805, Alcalá de Henares, Madrid, Spain

* Corresponding author: francisca.pina@uam.es

Abstract

The effect of nanoceria on two aquatic photosynthetic organisms of ecological relevance, a green alga and a cyanobacterium, is reported. The main bioenergetic process of these organisms, photosynthesis, was studied by measuring both oxygen evolution and chlorophyll *a* fluorescence emission parameters. Nanoceria significantly inhibited photosynthesis in the cyanobacterium in the entire range of concentrations tested (0.01–100 mg/L), while a dual effect of nanoceria was found in the green alga with slight stimulation at low concentrations and strong inhibition at the highest concentrations tested. Chlorophyll *a* fluorescence experiments indicated that nanoceria had a significant impact on the primary photochemical processes of photosystem II. The primary cause of the observed photosynthetic inhibition by nanoceria is an excessive level of ROS formation; the results indicated a strong generation of reactive oxygen species (ROS) which caused oxidative damage, as evidenced by lipid peroxidation in both photosynthetic organisms. It is proposed that nanoceria can increase the production of hydrogen peroxide (a normal ROS by-product of light-driven photosynthesis) in both the green alga and the cyanobacterium; through an oxidative reaction, these ROS cause lipid peroxidation, compromising membrane integrity and also seriously impairing photosynthetic performance, eventually leading to cell death.

Keywords: Antagonism; Cyanobacterium; Combination index; PFOA and PFOS; Synergism

1. Introduction

As a result of the rapid development of nanotechnology, the commercial applications of engineered nanoparticles (ENP) have expanded widely in recent years, leading to their subsequent increased release into the environment. The small size of ENP results in a larger surface area and enhanced reactivity in comparison with the same non-nano compounds raising concerns about their potential environmental and health risks (Tiede et al., 2009). Algae and cyanobacteria are abundant in aquatic ecosystems and interact strongly with their local environment; thus, both may be envisaged as ideal models to study any adverse effects of released ENPs. In addition, as these organisms are primary producers, occupying the lowest position in aquatic food chain networks and playing a key role in global biogeochemical cycles, any detrimental effects on them may result in an enhanced negative impact on organisms at higher trophic levels (Navarro et al., 2008).

Toxicological studies with most ENPs have revealed that their toxic action seems to involve the generation of ROS and the subsequent induction of cellular oxidative damage. In this regard, cerium oxide nanoparticles, which have widespread applications (Zhu et al., 2003), are interesting nanomaterials due to their unique redox properties which are based on the photocatalytic generation of electron–hole pairs.

It has been suggested that nanoceria act both as ROS producers and as antioxidants. Nanoceria are excellent oxygen buffers, exhibiting increased oxygen vacancies which permit redox cycles between the Ce(III) and the Ce(IV) oxidation states, and acting as free radical scavengers. In

DOI: 10.1016/j.aquatox.2012.06.005

addition, CeO_2 is capable of mimicking the behaviour of two key antioxidant enzymes, superoxide dismutase and catalase (Celardo et al., 2011, Das et al., 2007, Heckert et al., 2008, Korsvik et al., 2007), and most reports to date have found an antioxidant/protective effect of nanoceria in a variety of cellular systems (Chen et al., 2006, Schubert et al., 2006, Xia et al., 2008, Zhou et al., 2011). On the other hand, nanoceria, as well as other nanomaterials, are capable of spontaneous ROS production, they have been shown to catalyse a Fenton-like reaction in the presence of hydrogen peroxide (Xia et al., 2008, Zhang et al., 2011). In this regard, the number of studies which report oxidative damage following nanoceria exposure in a range of organisms, is also increasing (Kim et al., 2010, Lin et al., 2006, Park et al., 2008, Thill et al., 2006, Yokel et al., 2009, Zeyons et al., 2009, Zhang et al., 2011).

Our group previously showed that nanoceria exhibited strong toxicity to the green alga *Pseudokirchneriella subcapitata* and the cyanobacterium *Anabaena CPB4337*. In both organisms, nanoceria exposure resulted in highly damaged cells with extensive membrane disruption (Rodea-Palomares et al., 2011). The aim of the present study was to gain insights into the mechanisms of the observed toxicity. To this end, the effect of nanoceria on the main bioenergetic process of these organisms, photosynthesis, was studied by measuring both oxygen evolution and chlorophyll *a* fluorescence emission parameters. This latter technique is a non-destructive measure used to detect and estimate the status of photosystem II (PSII), which is the main site that is highly susceptible to many environmental stresses in photosynthetic organisms (Geoffroy et al., 2007, Papageorgiou et al., 2007). Although ROS are normal by-products of light-driven photosynthesis and cells keep them within tight margins (Apel and Hirt, 2004), photosynthesis is also one of the main cellular targets of oxidative damage. For this reason, we also examined the possibility of ROS generation and subsequent oxidative damage in the cells exposed to nanoceria.

2. Materials and methods

2.1. Materials

In this study, we used an uncoated CeO_2 (CAS No. 1306-38-3) nanopowder from Sigma–Aldrich. This material, denoted as N50, has a nominal particle size lower than 50 nm, which corresponds to a BET diameter of 22 nm (calculated assuming spherical particles) (Table 1). The size distribution of nanoparticles (<6000 nm) was obtained using dynamic light scattering (DLS, Malvern Zetasizer Nano ZS). High-resolution transmission electron microscopy (TEM) images of nanoparticles were taken on a JEOL (JEM-2000FX) microscope operating at 200 kV. Zeta potential was measured *via* electrophoretic light scattering combined with phase analysis light scattering in the same instrument equipped with a Malvern autotitrator MPT-2. The measurements were conducted at 25 °C using 10 mM in KCl as the dispersing medium.

Table 1. Physicochemical properties of CeO_2 nanoparticles

Size of primary particles (BET, nm)		22
BET surface area (m^2/g)		37.8
ζ-potential (mV)		
Pure water, 10 mM KCl, pH 8		-14.1 ± 0.4
OECD AGM, pH 8		-16.0 ± 0.9
AA/8+Nitrate, pH 7.5		-0.03 ± 0.16
Isoelectric point		+7.68 ± 0.25
	Growth media	
DLS size (nm)	OECD AGM, pH 8	AA/8+Nitrate, pH 7.5
1 mg/L	369 ± 54	416 ± 50
10 mg/L	858 ± 194	928 ± 122
50 mg/L	1298 ± 602	1399 ± 205
100 mg/L	1634 ± 463	1693 ± 992

2.2. Organisms and growth conditions

The filamentous cyanobacterium *Anabaena* CPB4337 was routinely grown at 28 °C in the light, Ca. 65 μmol photons m^2 s^{-1} on a rotary shaker in 50 mL AA/8 medium (Allen and Arnon, 1955) supplemented with nitrate (5 mM) in 125 mL Erlenmeyer flasks. The strain was grown in liquid cultures with 10 μg of neomycin sulphate (Nm) per mL. The toxicity experiments were carried out using 15 mL cultures grown in 25 mL Erlenmeyer flasks. Before nanoceria exposure, cultures were washed once with the culture medium and resuspended in fresh culture medium to obtain a final optical density ($OD_{750\ nm}$) of 0.3. Nanoparticles were added to obtain the desired exposure concentrations, and cultures were exposed to nanoceria for up to 72 h. *P. subcapitata* algae beads and culture media were purchased from Microbiotest Inc. The green alga was cultured in 50 mL flasks containing a total volume of 25 mL in OECD algal growth medium, as described in OECD TG 201, and mounted on a GFL 3005 orbital shaker. *P. subcapitata* cells were exposed for 72 h to the desired concentrations of CeO_2

DOI: 10.1016/j.aquatox.2012.06.005

nanoparticles, essentially as described previously (Rodea-Palomares et al., 2011). Experiments were carried out in a growing chamber with controlled temperature (at 22 °C), humidity and light intensity (~100 μmol photons m^{-2} s^{-1}).

2.3. Analytical methods

Cyanobacterial culture density was determined spectrophotometrically at 750 nm. For dry weight determinations, cells were collected, washed and dried at 70 °C for 24 h. Growth of *P. subcapitata* was monitored daily for 72/96 h and assessed by optical density (OD) at 640 nm using a microplate reader RAYTO RT-2100C and by direct cell counting using a Coulter Counter apparatus (2.5–8.5 μm). For cyanobacterial chlorophyll determinations, samples were extracted in methanol at 4 °C for 24 h in darkness. The chlorophyll content of the extract was estimated according to the spectrophotometric method of Marker (1972). For total chlorophyll determinations (chlorophyll *a* + *b*) of *P. Subcapitata*, samples were extracted in methanol at 4 °C for 24 h in darkness. The chlorophyll content of the extract was estimated according to the spectrophotometric method of Porra et al. (1989).

2.4. Photosynthetic oxygen evolution

Algal and cyanobacterial oxygen evolution was measured at 30 °C under saturating white light (300 μmol photons m^{-2} s^{-1}) with a Clark-type oxygen electrode (Hansatech, Kings Lynn, UK) as described elsewhere (Giraldez-Ruiz et al., 1997).

2.5. Chlorophyll a fluorescence emission measurements

Chlorophyll *a* fluorescence emission was measured with a pulse amplitude modulated (PAM) fluorometer (Hansatech FMS2, Hansatech, Inc, UK). After dark adaptation of cells for 30 min to completely oxidise the PSII electron transport chain, the minimum fluorescence (F_0; dark adapted minimum fluorescence) was measured with weak modulated irradiation (1 μmol m^{-2} s^{-1}). Maximum fluorescence (F_m) was determined for the dark adapted state by applying a 400 ms saturating flash (15800 μmol m^{-2} s^{-1}). In the case of the cyanobacterium, F_0 and F_m were assessed respectively before and after the addition of diuron and exposure to actinic light (Campbell et al., 1998, Deblois and Juneau, 2010). The diuron concentration used (5 μM final concentration) was that necessary to permit the reduction of all PSII reaction centres, since increasing the saturating flash did not allow a further increase in F_m. The variable fluorescence (F_v) was calculated as the difference between the maximum fluorescence (F_m) and the minimum fluorescence (F_0). The maximum photosynthetic efficiency of photosystem II (maximal PSII quantum yield) was calculated as F_v/F_m. During the saturation flash, the cells were continuously irradiated with red–blue actinic beams [the actinic light was adjusted to match photon irradiances of the growth chamber for each organism (200 μmol m^{-2} s^{-1} and 260 μmol m^{-2} s^{-1} for the cyanobacterium and alga, respectively)] and equilibrated for 60 s to record F_s (steady-state fluorescence signal). Following this, another saturation flash (15800 μmol m^{-2} s^{-1} during 0.4 s) was applied and then F_m' (maximum fluorescence under light adapted conditions) was determined; afterwards, the actinic source was automatically switched off, a 5 s far-red pulse was applied and the minimum fluorescence yield stored as F_0'. Other fluorescent parameters were calculated as follows: the effective PSII quantum yield $\Phi PSII = (F_m' - F_s)/F_m'$ (Genty et al., 1989), intrinsic PSII efficiency $F_v'/F_m' = (F_m' - F_0')/F_m'$, the photochemical quenching coefficient $qP = (F_m' - F_s)/(F_m' - F_0)$, the non-photochemical quenching coefficient $NPQ = (F_m - F_m')/F_m'$, the vitality index $Rdf = (F_m - F_s)/F_s$ and the electron transport rate $ETR = \Phi PSII \times PAR \times 0.5 \times 0.85$.

2.6. Flow cytometric analyses

Chlorophyll (cell autofluorescence), esterase activity and lipid peroxidation were evaluated using a Cytomix FL500 MPL flow cytometer (Beckman Coulter Inc., Fullerton, CA, USA) equipped with an argon-ion excitation wavelength (488 nm), detector of forward (FS) and side (SS) light scatter and four fluorescence detectors corresponding to four different wavelength intervals: FL1:525, FL2:575, FL3:620 and FL4: 675 (±20 nm). Before each experiment, settings were adjusted. The flow rate was set at 1 μL s^{-1} and at least 20,000 events (algal cells or cyanobacterial filaments) were counted. Non-algal/cyanobacterial particles were excluded from the analysis by setting an acquisition threshold value (1) for the forward-scatter (FS) parameter. Light scattered by cells is collected at two angles: FS and SS. Forward scatter measures scattered light in the direction of the laser path and provides data on cell size. Side scatter measures scattered light at 90° to the laser path and provides information on the complexity (internal granularity) of the cell; it is used to determine the

DOI: 10.1016/j.aquatox.2012.06.005

granular content of cells. Side and forward-scattered light are used in combination to distinguish between different cell types/populations.

The assessment of ROS generation was accomplished by loading cultures of control and treated cells with the fluorescent dye 2′,7′-dichlorofluorescein diacetate (H_2DCFDA) (Invitrogen Molecular Probes; Eugene, OR, USA). This compound diffuses into the cells where it is converted to its non-fluorescent form 2,7-dichlorodihydrofluorescein (H_2DCF) by cellular esterases. The oxidation of 2,7-dichlorodihydrofluorescein originates 2,7-dichlorofluorescein (DCF), a fluorescent compound that serves as an indicator for hydrogen peroxide and other ROS, such as hydroxyl and peroxyl radicals (Gomes et al., 2005). A 10 mM H_2DCFDA stock solution was freshly prepared in DMSO under dim light conditions to avoid its degradation. Prior to flow cytometric analysis, the cyanobacterium and the green alga were incubated for 10 min at room temperature with a final concentration of 1 μM (cyanobacterium) or 10 μM (green alga) H_2DCFDA. As a positive control for ROS formation, 3% H_2O_2 (v/v) and 2.5% ethanol (v/v) (final concentrations) were added to algal and cyanobacterial cells, respectively.

C4-BODIPY® was used for evaluating lipid peroxidation since it is susceptible to oxidation by peroxyl radicals, producing green fluorescence. A 0.5 mM C4-BODIPY® stock solution was freshly prepared in methanol under dim light conditions to avoid its degradation. Prior to flow cytometric analysis, the cyanobacterium and the green alga were incubated for 10 min at room temperature with a final concentration of C4-BODIPY® of 2.5 μM for the cyanobacterium and 5 μM for green alga. As a positive control, 0.5% ethanol (v/v) and 3% H_2O_2 (final concentrations) were added to algal and cyanobacterial cells, respectively.

Chlorophyll red autofluorescence was collected with a 610 nm long band pass filter (FL4), DCF and C4-BODIPY® green fluorescence was collected with the 530/30 nm band pass filter (FL1). Data acquisition was performed using MXP-2.2 software, and the analyses were performed using CXP-2.2 analysis software. Fluorescence was analysed in Log mode.

2.7. Confocal microscopy

DCF, chlorophyll *a* and C4-BODIPY® fluorescence in cells were visualised using a confocal fluorescence microscope (Leica TCS SP5) with excitation at 488 nm; chlorophyll/DCF and chlorophyll/C4-BODIPY® emissions were simultaneously recorded at 665 nm and 535 nm, respectively.

2.8. Reproducibility and analysis of results

At least three independent experiments with duplicate samples were carried out; measurements were always performed in duplicate. All tests of statistically significant differences between datasets were performed using Student's *t*-tests at $P < 0.05$ with MINITAB Release 14 software for Windows (Minitab Inc; USA). In the flow cytometry analyses, differences between cell subpopulations were assessed by the Kolmogorov–Smirnov test ($P < 0.05$) using CXP-2.2 software.

3. Results

3.1. Characteristics of nanoparticles

The characteristics of the nanoceria in the growth media tested are presented in Table 1. It is interesting to note that the nanoparticles bear a negative charge at pH 8, while being neutral at pH 7.5, close to the isoelectric point of the oxide. The size of aggregates increased with mass concentration, reaching micron size above 10 mg/L in both media; TEM images of large aggregates of nanoparticles at 100 mg/L are shown as Supplementary Information (Fig. S1). DLS measurement of hydrodynamic size gave stable readings for at least two weeks following preparation of the suspension, as indicated elsewhere (Rodea-Palomares et al., 2011). In addition, we have previously shown that nanoparticle aggregates included cyanobacterial and algal cells, particularly at high nanoceria concentrations (Rodea-Palomares et al., 2011). The amount of dissolved metals in the growth media tested was previously assessed by performing Inductively coupled plasma-mass spectrometry analyses (CP-MS Elan 6000 PerkinElmer Sciex) on samples ultrafiltrated by 10 kDa MWCO Vivaspin 6 Centrifugal tubes. The results indicated negligible (< 0.1 μg/L for 100 mg/L CeO2) amounts of dissolved Ce which did not contribute to the toxicological effects observed (Rodea-Palomares et al., 2011).

3.2. Photosynthetic responses of Anabaena CPB4337 and Pseudokirchneriella subcapitata to nanoceria

The effect of nanoceria in the concentration range 0.01–100 mg/L on the photosynthesis of both the

DOI: 10.1016/j.aquatox.2012.06.005

cyanobacterium and the green alga, measured as oxygen evolution, is shown in Fig. 1; chlorophyll contents are also shown in the figure. Cyanobacterial photosynthetic oxygen evolution significantly (Student's t-test, $P < 0.05$) decreased with nanoceria concentrations higher than 1 mg/L (Fig. 1A). Chlorophyll content increased slightly in cyanobacterial cells for the entire range of nanoceria concentrations. In contract, the photosynthetic oxygen evolution of the green alga exposed to nanoceria showed a dual response, with an increase which ranged between 20% and 50% of the control value when exposed to low nanoceria concentrations in the 0.01–1 mg/L range, and a significant (Student's t-test, $P < 0.05$) decrease at higher concentrations (Fig. 1B); the observed decrease was slightly higher than the one observed for the cyanobacterium at the same nanoceria concentrations. Chlorophyll content per cell exhibited a significant (Student's t-test, $P < 0.05$) decrease in the range 0.1–100 mg/L.

To gain an insight into the mechanisms of the effects of nanoceria on photosynthesis in both the cyanobacterium and the green alga, we performed chlorophyll fluorescence emission analyses which enabled us to determine the photochemical reactions of photosynthesis, efficiency of photosystem II and electron transport rate. In the concentration range 0.01–100 mg/L, the effect of nanoceria on the main chlorophyll fluorescence parameters of both the cyanobacterium and the green alga is shown in Table 2; for the green alga, an intermediate concentration of 50 mg/L was included due to the fact that, as shown below, the most significant differences were found at 100 mg/L. The F_0 parameter, fluorescence levels when the plastoquinone electron acceptor pool (Q_A) is fully oxidised, is a sensitive indicator of stress in plants (Fracheboud et al., 2004). It represents the emission of excited antenna chlorophyll *a* molecules before the excitation migrates to the reaction centres and is independent of photochemical events; it may be considered an estimate of the relative size of the antenna of the PSII complex (Krause and Weis, 1991). Nanoceria at the lowest concentration tested significantly (Student's *t*-test, $P < 0.05$) increased F_0 in the cyanobacterium, producing an increase of 30% with respect to the control at the highest concentrations tested. The effect on F_0 in the green alga was somewhat different, as a significant (Student's *t*-test, $P < 0.05$) although slight decrease was found at relatively low nanoceria concentrations and a significant (Student's *t*-test, $P < 0.05$) increase was observed at the highest concentrations tested (45% with respect to the control at 100 mg/L). It should be noted that in the green alga, F_0 decreased at nanoceria concentrations where the stimulatory effect on photosynthetic oxygen evolution was recorded (Fig. 1B).

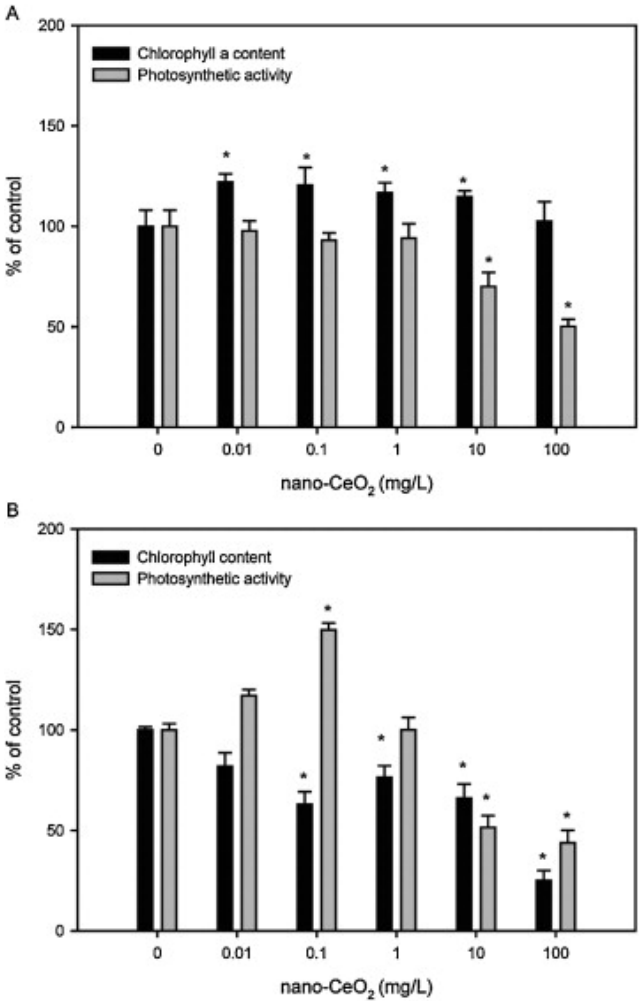

Figure 1. Effect of 72 h exposure to CeO_2 nanoparticles on photosynthetic activity and chlorophyll content of *Anabaena* CPB4337 (A) and *P. Subcapitata* (B). All data are presented as the percent of corresponding control samples. Data are mean ± C.I. (95% confidence interval) ($n = 3$). Significant differences at $P < 0.05$ between control and treated cultures are marked by asterisks.

Nanoceria significantly (Student's *t*-test, $P < 0.05$) decreased dark adapted maximum fluorescence, F_m, at all tested concentrations in the cyanobacterium, with a maximum decrease of around 30% at the lowest concentrations. In the case of the green alga, a significant (Student's *t*-test, $P < 0.05$) decrease was observed only in the 0.1–10 mg/L range, with a maximum decrease of 21% at 1 mg/L. The observed decrease in F_m was

DOI: 10.1016/j.aquatox.2012.06.005

Table 2. Chlorophyll a fluorescence parameters of *Anabaena* CPB4337 and *P. Subcapitata* exposed for 72h to CeO_2 nanoparticles.

Anabaena CPB4337 (72h)							
	CeO_2-nanoparticle (mg/L)						
	control	0.01	0.1	1	10	50	100
Fo	56.7 ± 3.4	66.0 ± 9.6*	64.0 ± 3.2*	67.5 ± 0.8*	77.50 ± 2.40*	Nd	70.0 ± 12.8
Fm	239 ± 10	157.5 ± 8.8*	160.5 ± 4.0*	158.0 ± 3.2*	180.5 ± 4.0*	Nd	170.5 ± 29.6*
Fs	99.5 ± 6.9	113.5 ± 8.8*	141.5 ± 2.4*	139 ±17*	143.5 ± 7.2*	Nd	169.0 ± 32.0*
Rdf	1.52 ± 0.46	1.23 ± 0.04	0.81 ± 0.03*	0.67 ± 0.11*	0.77 ± 0.02*	Nd	0.59 ± 0.06*
Fv/Fm	0.76 ± 0.02	0.74 ± 0.01	0.75 ± 0.01	0.70 ± 0.01*	0.69 ± 0.02*	Nd	0.74 ± 0.01
ϕPSII	0.42 ± 0.02	0.37 ± 0.01	0.34 ± 0.01*	0.29 ± 0.03*	0.34 ± 0.04*	Nd	0.21 ± 0.02*
qP	0.63 ± 0.04	0.59 ± 0.03	0.48 ± 0.01*	0.44 ± 0.06*	0.53 ± 0.01*	Nd	0.31 ± 0.03*
Fv`/Fm`	0.52 ± 0.01	0.48 ± 0.01*	0.43 ± 0.01*	0.41 ± 0.02*	0.45 ± 0.01*	Nd	0.37 ± 0.05*
NPQ	0.42 ± 0.08	0.38 ± 0.01	0.19 ± 0.01*	0.18 ± 0.02*	0.15 ± 0.01*	Nd	0.25 ± 0.01*
ETR	35.6 ± 3.3	31.7 ± 0.7	28.6 ± 0.5*	24.5 ± 2.6*	29.2 ± 0.3*	Nd	18.1 ± 2.2*
P. Subcapitata (72h)							
	CeO_2-nanoparticle (mg/L)						
	control	0.01	0.1	1	10	50	100
Fo	14.8 ± 0.4	15.0 ± 0.5	13.5 ± 0.5*	10.5 ± 0.5*	13.5 ± 0.5*	19.2 ± 2.5*	21.5 ± 0.5*
Fm	78.2 ± 3.5	71.5 ± 4.3	72.2 ± 2.4*	61.2 ± 3.2*	76.5 ± 4.4	88.2 ± 4.1*	88.2 ± 5.2*
Fs	16.2 ± 0.4	15.5 ± 0.5	15.2 ± 0.4	12.2 ± 0.4*	17.2 ± 0.9	35.0 ± 3.4*	34.5 ± 3.0*
Rdf	3.7 ± 0.2	3.62± 0.3	3.7 ± 0.1	4.0 ± 0.1	3.4 ± 0.3	1.5 ± 0.1*	1.5 ± 0.1*
Fv/Fm	0.81 ± 0.01	0.79 ± 0.01	0.81 ±	0.82 ± 0.01*	0.82 ± 0.01	0.78 ± 0.02*	0.75 ± 0.01*
ϕPSII	0.67 ± 0.03	0.69 ± 0.02	0.69 ± 0.01	0.70 ± 0.03	0.64 ± 0.01*	0.49 ± 0.02*	0.59 ± 0.02*
qP	0.86 ± 0.03	0.86 ± 0.01	0.87 ± 0.01	0.86 ± 0.01	0.82 ± 0.01*	0.71 ± 0.01*	0.77 ± 0.01*
Fv`/Fm`	0.78 ± 0.01	0.80 ± 0.02	0.79 ± 0.01	0.81 ± 0.03	0.78 ± 0.01	0.69 ± 0.01*	0.76 ± 0.01*
NQP	0.56 ± 0.17	0.49 ± 0.08	0.47 ± 0.04	0.50 ± 0.14	0.57 ± 0.09	0.27 ± 0.03*	0.04 ± 0.01*
ETR	56.4 ± 2.1	57.6 ± 1.6	58.3 ± 0.4	59.2 ± 2.6	54.2 ± 2.1	41.6 ± 1.5*	49.7 ± 1.7*

Data are means ± C.I. (95% Confidence Interval) (n=3) Significant differences at $P < 0.05$ between control and treated cultures are marked by asterisks.

in agreement with the observed significant (Student's *t*-test, $P < 0.05$) increase in F_s, a parameter which increases when closed/reduced (non-active) PSII centres increase. The rise in this parameter was significant in all the tested concentrations in the cyanobacterium, with an increase of nearly 70% at the highest concentration, 100 mg/L. In the green alga there was a decrease at concentrations ranging from 0.01 to 1 mg/L, which again correlated with the concentrations of higher photosynthetic activity (Fig. 1B), and an increase was only evident at the highest concentrations tested, 50 and 100 mg/L (more than 100% increase).

The parameter Rdf, $(F_m - F_s)/F_s$, also termed the "vitality index", is widely accepted as a measure of stress effects on PSII (Roháček, 2002). As shown in the table, a significant (Student's *t*-test, $P < 0.05$) decrease in this index was observed in the cyanobacterium at nanoceria concentrations of 0.1 mg/L and above, with a maximum decrease of 60% at 100 mg/L. In the green alga, a significant (Student's *t*-test, $P < 0.05$) decrease (also around 60%) was only found at the highest concentrations tested, 50 and 100 mg/L.

The dark adapted F_v/F_m ratio is used as an indicator of maximum photosynthetic performance, particularly useful under photoinhibition and photodamage (Roháček, 2002). It reflects the potential maximum of PSII quantum yield or quantum efficiency of open PSII centres (Maxwell and Johnson, 2000). As shown in the table, nanoceria slightly decreased this ratio in the cyanobacterium, this decrease was clearly significant (Student's *t*-test, $P < 0.05$) only at 1 and 10 mg/L. In the green alga, the behaviour was again dual: this parameter initially increased at low nanoceria concentrations and a decrease, significant (Student's *t*-test, $P < 0.05$) although very modest, was found at 50 and 100 mg/L. As neither a gradual nor an important decrease was found for this parameter, it seems that F_v/F_m is not

a sensitive indicator of nanoceria toxicity in either of the two organisms.

The effective quantum yield of PSII, ΦPSII, is used as a general indicator of plant stress physiology (Genty et al., 1989). This ratio is an estimate of the effective portion of absorbed quanta used in PSII reaction centres: it is affected by the proportion of open, oxidised PSII reaction centres (estimated by the so-called photochemical quenching or qP) and also by the intrinsic PSII efficiency (estimated as the F_v'/F_m' ratio) (Genty et al., 1989). As shown in Table 2, nanoceria exposure significantly (Student's *t*-test, $P < 0.05$) decreased ΦPSII in both the cyanobacterium and the green alga: in the cyanobacterium, the decrease was observed at all the tested concentrations with a maximum decrease of nearly 50% at the highest concentration tested, 100 mg/L, whereas in the green alga, a significant (Student's *t*-test, $P < 0.05$) decrease was observed at 10, 50 and 100 mg/L with a maximum of 26% at 50 mg/L. In both organisms, the observed decrease in this parameter at the above-mentioned concentrations correlated very well with corresponding decreases in photochemical quenching, qP, and the intrinsic PSII efficiency, F_v'/F_m'. In the cyanobacterium, the qP decrease was significant (Student's *t*-test, $P < 0.05$) at concentrations of 0.1 mg/L and above, with a maximum decrease of 50% at 100 mg/L, whereas in the green alga the decrease was modest (10% maximum) and only significant (Student's *t*-test, $P < 0.05$) at 10, 50 and 100 mg/L.

The decrease in F_v'/F_m' followed the same pattern as that of qP in both organisms: in the cyanobacterium, a significant (Student's *t*-test, $P < 0.05$) decrease was evident at low nanoceria concentrations while in the green alga, the decrease occurred at the highest concentrations tested. A decrease in F_v'/F_m' may be caused by any defect in the quantum yield of PSII itself, such as non-photochemical quenching, NPQ. As shown in the table, this parameter significantly (Student's *t*-test, $P < 0.05$) decreased in both organisms and as with several of the above-mentioned parameters, the decrease in the cyanobacterium was already significant (Student's *t*-test, $P < 0.05$) at 0.1 mg/L, with a maximum decrease of 62% at 10 mg/L, while in the green alga, the decrease was significant (Student's *t*-test, $P < 0.05$) only at 50 and 100 mg/L. However, it should be mentioned that a drastic decrease of around 92% in this parameter was found at 100 mg/L nanoceria in the green alga.

The linear electronic transport rate, ETR, can be calculated from ΦPSII (Genty et al., 1989). As shown in the table, the ETR decreased in agreement with the decreases observed in ΦPSII in both organisms, with a maximum decrease of around 50% at 100 mg/L for the cyanobacterium and a more modest decrease in the green alga (26% maximum decrease at 50 mg/L).

3.3. ROS generation in Anabaena CPB4337 and Pseudokirchneriella subcapitata due to nanoceria exposure

The primary cause of the observed photosynthetic inhibition by nanoceria in both organisms could be an excessive level of ROS formation. ROS generation and subsequent oxidative stress was evaluated by using the fluorescence indicators H_2DCFDA (general oxidative stress indicator) and C4-BODIPY® (lipid peroxidation indicator) in flow cytometry and confocal microscopy studies.

Fig. 2 shows flow cytograms of cell/filament complexity (internal granularity) as a function of cell/filament size of *Anabaena* CPB4337 and *P. subcapitata* exposed to CeO_2 nanoparticles. As shown in Fig. 2, nanoceria exposure increased cell size and complexity in both the alga and cyanobacterium (AI cell/filament subpopulation), although this change in complexity and size was greater in the alga than in the cyanobacterium and clearly dependant on nanoceria concentrations. The increase in cell complexity, particularly in the alga, may be due to the formation of particle aggregates which include algal cells (Rodea-Palomares et al., 2011). The AI cell/filament subpopulation denoted as *N* showed the greatest size and complexity in both organisms, and this subpopulation clearly diminished upon exposure to the higher nanoceria concentrations. It is also evident in the figure that at nanoceria concentrations of 10 mg/L and above for the cyanobacterium, and in the concentration range 1–100 mg/L for the alga, there is a significant shift to the left indicating a subpopulation of cells, denoted as *J* (which reaches 89% total cells in the cyanobacterium and 71% total cells in the alga at 100 mg/L nanoceria), with diminished cell size/complexity which might indicate highly damaged cells or even cell death and lysis induced by nanoceria exposure (Rodea-Palomares et al., 2011).

Fig. 3 shows density plots of DCF, BODIPY and chlorophyll fluorescence *vs* size for *Anabaena* CPB4337 (A) and *P. subcapitata* (B). The intensity pattern of the density plots (from blue, meaning low intensity, to red, meaning high intensity)

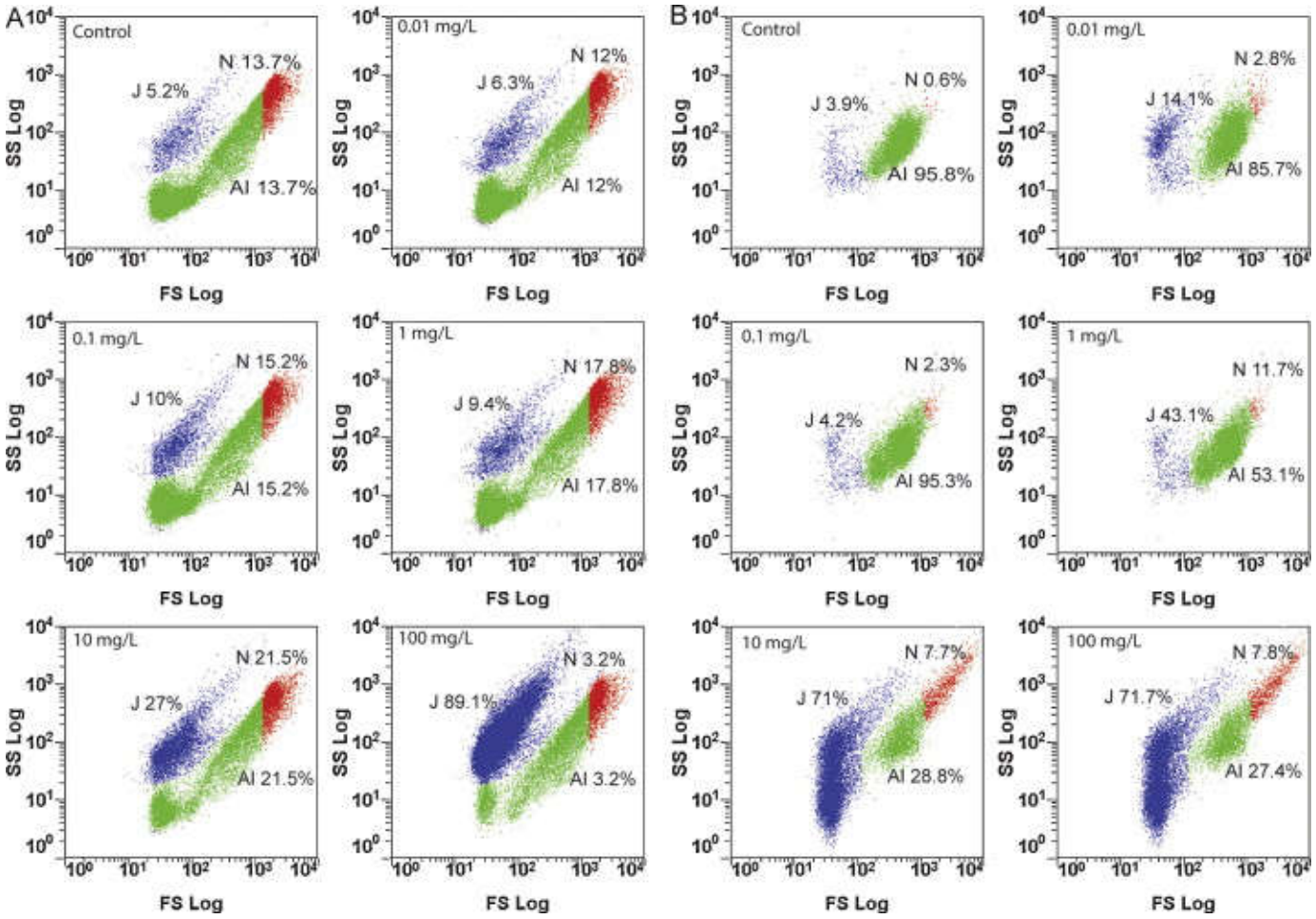

Figure 2. Flow cytograms of cell/filament complexity (SS) as a function of cell/filament size (FS) of *Anabaena* CPB4337 (A) and *P. subcapitata* (B) exposed for 72 h to CeO_2 nanoparticles. Cell/filament subpopulations were identified based on size and complexity: AI = main subpopulation (green dots), *N* = AI subpopulation which included cells/filaments with the highest size and complexity (red dots) and *J* = cells/filaments with the smallest size/complexity and/or cell debris (blue dots). Percentages of total events in each population are included in the figures.

denoted the number of events (cells/filaments) with the same size and fluorescence intensity values. Table 3 shows DCF, BODIPY and chlorophyll average fluorescence intensity values (as a percentage with respect to the control) for the main cell/filament subpopulations established in the flow cytograms (Fig. 2) and density plots (Fig. 3) for *Anabaena* CPB4337 and *P. subcapitata* exposed for 72 h to CeO_2 nanoparticles.

As shown in Fig. 3 and Table 3, nanoceria exposure induced an increase in DCF fluorescence in both the alga and the cyanobacterium, and this increase was apparent from the lowest nanoceria concentration, 0.01 mg/L already indicating oxidative stress in both organisms at low nanoceria concentrations. The increase reached almost 500% and 700% with respect to the control in the AI cell subpopulation at 100 mg/L in the cyanobacterium and the alga, respectively (Table 3), and the AI cell subpopulation denoted as *N* showed the highest DCF fluorescence intensity values in the presence of nanoceria (Table 3 and Fig. 3). As regards the *J* subpopulation, which, as outlined above, most probably represents highly damaged cells and cell debris, DCF fluorescence intensity values were already very low in the cyanobacterium (see Table 3) although they increased to 400% of *J* control values at 1 mg/L nanoceria and decreased to around 270% at 100 mg/L, whereas in the green alga, the maximum increase in the *J* subpopulation was observed at 100 mg/L reaching 140% of the control value (Table 3).

Fig. 4 shows confocal micrographs of DCF green fluorescence and chlorophyll red autofluorescence of both organisms exposed to 10 mg/L of nanoceria. As can be seen, there is an evident increase in ROS generation by nanoceria in all cells of the cyanobacterial filament (Fig. 4A), cells which are viable as shown by the red chlorophyll autofluorescence; however the fluorescence is not

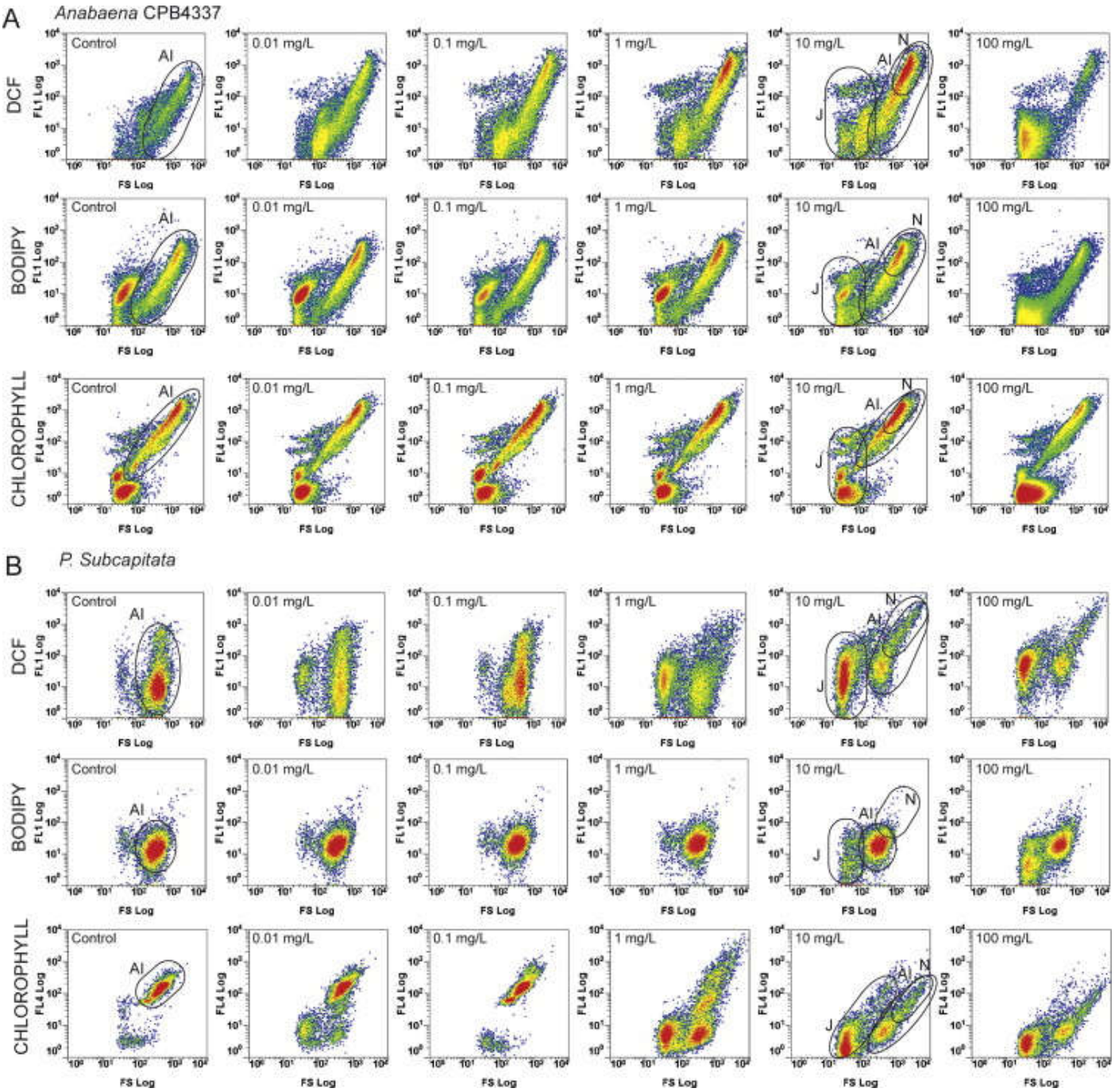

Figure 3. Flow cytometry density plots depicting DCF fluorescence, BODIPY fluorescence and chlorophyll fluorescence intensity *vs* size (FS) of *Anabaena* CPB4337 (A) and *P. subcapitata* (B) exposed for 72 h to CeO_2 nanoparticles. The intensity pattern of the density plots (from blue, meaning low intensity, to red, meaning high intensity) denoted the number of events (cells/filaments) with the same size and fluorescence intensity values. Main cell/filament subpopulations AI, *J* and *N* (see Fig. 2) are marked.

uniform, and there are cytoplasmic spots with increased fluorescence that are clearly seen in theoverlay micrograph of the red cyanobacterial autofluorescence and the green DCF fluorescence. In the case of the green alga (Fig. 4B), DCF fluorescence is only observed in damaged, tiny cells (as shown by the lack of red autofluorescence; see the overlay micrograph) in close contact with what could be nanoparticle/cell debris aggregates (Rodea-Palomares et al., 2011).

BODIPY fluorescence increased in the cyanobacterium at 1 and 10 mg/L nanoceria (Fig. 3A and Table 3), particularly in the AI cell subpopulation, with a maximum increase of 150% at 1 mg/L, indicating lipid peroxidation in this range of concentrations: at the highest concentration, 100 mg/L, BODIPY fluorescence decreased in all cell subpopulations (see Table 3). Fig. 5 shows confocal micrographs of BODIPY green fluorescence and chlorophyll red autofluorescence of both organisms exposed to 10

Table 3. DCF, BODIPY and chlorophyll average fluorescence intensity values as a percentage with respect to the control of the main cell/filament subpopulations established in the flow cytograms (Figure 2) for *Anabaena* CPB4337 and *P. subcapitata* exposed for 72 h to CeO_2 nanoparticles.

Anabaena CPB4337												
Fluorescence intensity (%)												
[CeO_2]	DCF fluorescence (FL1)				BODIPY fluorescence (FL1)				Chlorophyll fluorescence (FL4)			
mg/L	All	AI	N	J	All	AI	N	J	All	AI	N	J
0	100.0 (37.5)[1]	100.0 (96.3)[1]	100.0 (244.1)[1]	100.0 (2.57)[1]	100.0 (40.7)[1]	100.0 (83.9)[1]	100.0 (212.2)[1]	100.0 (11.1)[1]	100.0 (152.2)[1]	100.0 (418.9)[1]	100.0 (995.7)[1]	100.0 (6.7)[1]
0.01	107.2	196.3	191.0	133.9	91.9	107.4	93.9	87.1	46.5	79.7	73.0	91.9
0.1	249.3	289.7	248.0	261.5	105.9	106.8	96.2	72.2	91.4	100.7	82.9	120.4
1	437.3	468.3	279.9	408.6	149.9	150.2	109.4	100.9	134.9	137.8	83.5	131.9
10	341.3	461.1	278.7	339.7	161.7	139.5	103.8	88.7	109.2	139.0	85.3	147.7
100	132.8	496.4	288.5	276.7	23.6	101.7	93.9	16.4	40.6	153.8	90.8	64.5
P. subcapitata												
Fluorescence intensity (%)												
[CeO_2]	DCF fluorescence (FL1)				BODIPY fluorescence (FL1)				Chlorophyll fluorescence (FL4)			
mg/L	All	AI	N	J	All	AI	N	J	All	AI	N	J
0	100.0 (39.6)[1]	100.0 (39.8)[1]	100.0 (345.0)[1]	100.0 (45.4)[1]	100.0 (17.8)[1]	100.0 (17.4)[1]	100.0 (64.5)[1]	100.0 (27.7)[1]	100.0 (142.7)[1]	100.0 (148.0)[1]	100.0 (195.6)[1]	100.0 (16.1)[1]
0.01	162.9	175.4	87.0	78.0	135.4	165.5	97.4	143.3	92.3	102.7	105.1	52.4
0.1	156.8	161.3	80.3	68.7	142.7	142.5	90.4	162.1	109.9	111.5	129.7	41.2
1	104.8	137.2	116.8	55.1	153.4	154.0	90.7	143.3	47.5	77.7	288.2	38.8
10	303.0	157.5	158.3	105.3	116.3	129.9	91.3	70.8	8.3	19.6	21.9	25.9
100	328.3	713.6	137.7	143.8	98.3	136.8	97.2	45.8	6.2	14.1	13.1	23.1

All: Total cell/filament subpopulation; AI: Main cell/filament subpopulation; N: AI subpopulation with the highest size and complexity; J: Smallest- size subpopulation with low chlorophyll autofluorescence signal which may include damaged cells/cell debris due to CeO_2 nanoparticles exposure. [1]: Mean fluorescence intensity values (arbitrary units) of the indicated cell/filament subpopulation in the control samples.

mg/L of nanoceria. As can be seen in the figure (Fig. 5A), confocal microscopy depicts a clear and significant increase in BODIPY fluorescence in all cells of the cyanobacterial filaments exposed to 10 mg/L nanoceria. Cells are viable, as shown by the red autofluorescence: however, the cellular distribution of BODIPY fluorescence is quite uniform (see also the overlay micrograph) compared with DCF fluorescence (Fig. 4A). In the green alga, nanoceria increased BODIPY green fluorescence in the AI subpopulation, with values around 150% in the concentration range between 0.01 and 1 mg/L, *L* indicating lipid peroxidation in this range of concentrations: above this value, fluorescence intensity decreased (Fig. 3B and Table 3). In the *J* subpopulation, there was also a similar increase in BODIPY green fluorescence in the same nanoceria concentration range (Fig. 3B and Table 3). Confocal microscopy (Fig. 5B) shows that BODIPY fluorescence induced by 10 mg/L nanoceria is generated mainly in cells which are aggregated, possibly with nanoparticles/cell debris, although as shown by the overlay micrograph some of these cells are still viable as they maintain red autofluorescence.

Density plots of chlorophyll red autofluorescence *vs* size are also shown in Fig. 3. In the cyanobacterium (Fig. 3A), chlorophyll red autofluorescence increased slightly in the AI subpopulation for the entire range of nanoceria concentrations, and this may be related to the observed increase in chlorophyll content in the cyanobacterium (Fig. 1A). However, it was very low in the *J* subpopulation which, as already mentioned, most probably indicates highly damaged or even lysed and dead cells (see Table 3). In the green alga, the autofluorescence signals clearly decreased at concentrations above 0.1 mg/L in all cell subpopulations (see Fig. 1B), particularly in the *J* subpopulation indicating highly damaged cells/cell debris: these results agree with the absence of autofluorescence in many of the aggregated cells observed in the confocal micrographs (Figs. 4B and 5B).

4. Discussion

To the best of our knowledge, this is the first report in the literature concerning the effect of nanoceria on photosynthesis; the available reports address on the effect of Ce (III) on the protection of photosynthesis of plants exposed to different types of stress (Liang et al., 2011, Yuguan et al., 2009, Zhou et al., 2011). It should be noted that while the effect of nanoceria on the cyanobacterium was

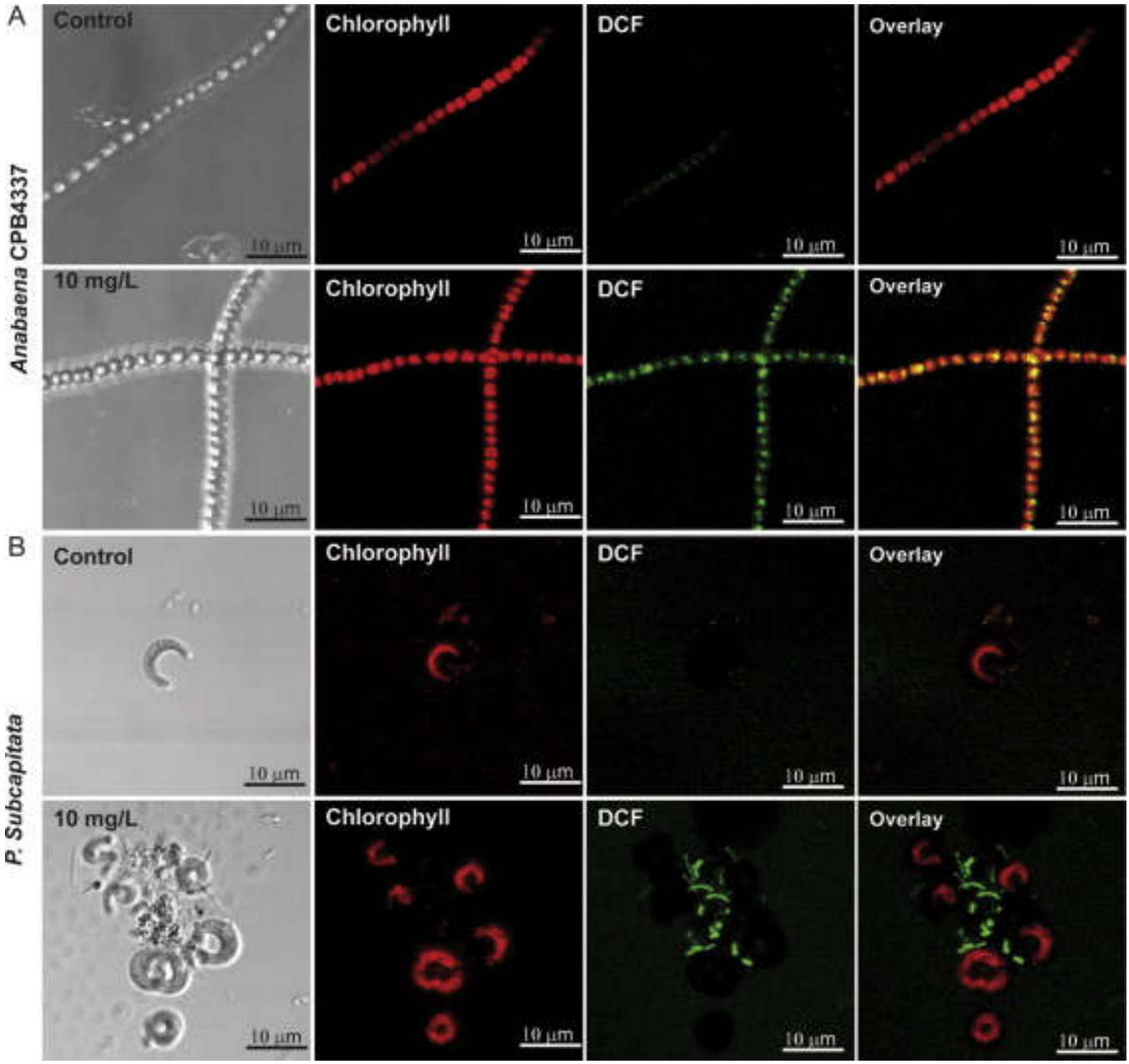

Figure 4. Confocal microscopy images of *Anabaena* CPB4337 (A) and *P. subcapitata* (B) exposed for 72 h to 10 mg/L CeO_2 nanoparticles showing intracellular green DCF fluorescence as a result of ROS production. Red fluorescence: chlorophyll autofluorescence; green fluorescence: DCF fluorescence; yellow fluorescence: overlay image of chlorophyll red autofluorescence and DCF green fluorescence.

clearly toxic, with a significant inhibition of photosynthesis, in the green alga the effect was dual, with a stimulation of photosynthesis at relatively low nanoceria concentrations and a significant inhibition at the highest concentrations tested. This particular behaviour suggests a hormetic dose–response (Calabrese, 2008) but should be studied further.

Chlorophyll fluorescence parameters may be used as indicators of stress affecting photochemical pathways and utilisation of absorbed light energy since they provide information on the location of the primary site of photosynthesis damage induced by environmental pollution (Fai et al., 2007, Kummerová et al., 2006, Pan et al., 2008). An increase in F_0 is characteristic of the destruction of PSII reaction centres (damage to D1 protein and other reaction centre components) or the impairment of transfer of excitation energy from antennae to the reaction centres in higher plants (Björkman and Demmig, 1987). In these organisms, an increase in this parameter is usually associated with detachment of the light harvesting complexes (antennae) from the PSII core, and thus an increase in the background fluorescence, F_0, should be expected (Armond et al., 1980, Havaux,

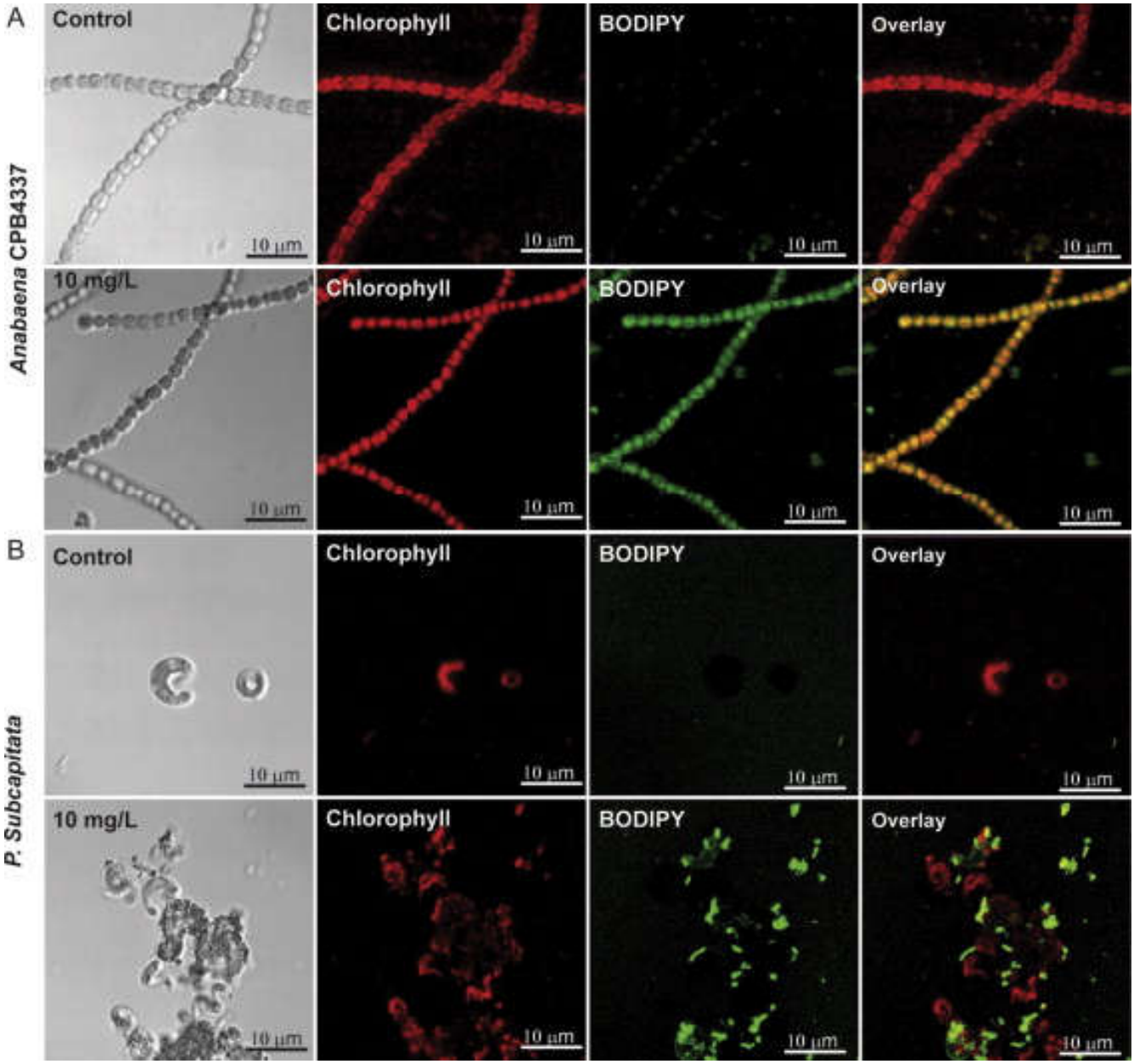

Figure 5. Confocal microscopy images of *Anabaena* CPB4337 (A) and *P. subcapitata* (B) exposed for 72 h to 10 mg/L CeO_2 nanoparticles showing intracellular green BODIPY fluorescence as a result of lipid peroxidation. Red fluorescence: chlorophyll autofluorescence; green fluorescence: BODIPY fluorescence; yellow fluorescence: overlay image of chlorophyll red autofluorescence and BODIPY green fluorescence.

1993, Kummerová et al., 2006). The destruction of photosynthetic pigments has also been suggested as the mechanism for an increase in F_0 in plants exposed to pollutants such as PAHs (Kummerová et al., 2006). As shown earlier, no decrease in chlorophyll content was observed in the cyanobacterium although this was evident in the green alga at concentrations above 0.1 mg/L (Fig. 1B). In addition, a decrease in efficiency from detached antennae complexes to the reaction centres of PSII or even a destruction of the reaction centres could also be the reason for the observed effect on F_0. Regarding F_m, an increase in closed/reduced PSII reaction centres which do not participate in electron transport may explain the observed decrease in this parameter (Pan et al., 2008, Toth et al., 2005). Furthermore, the observed decrease in F_m correlates with the increase in F_s, which indicates an increase in the number of non-active PSII centres, and this is further supported by the observed and significant decrease in qP in both organisms, which indicates that the number of open/active PSII centres are diminished upon exposure to nanoceria. NPQ reflects heat-dissipation of excitation energy in the antennae system and is a combination of photoprotective mechanisms, state 1 and state 2 transitions, photoinhibition and photodamage (Krause and Weis, 1991). During photosynthesis inhibition, NPQ increases in order to avoid

DOI: 10.1016/j.aquatox.2012.06.005

photodamage (Geoffroy et al., 2003). However, a decrease in NPQ may indicate damage in the antennae pigments where NPQ takes place. This parameter is considered a very sensitive indicator of photosynthetic malfunction (Fai et al., 2007, Ricart et al., 2010). In this respect, the relevant and significant overall decrease in the Rdf parameter in both organisms is a further indication of damage in PSII. According to the chlorophyll fluorescence analyses, there were some differences in the toxic effect of nanoceria on both types of photosynthetic organisms: in the cyanobacterium, most of the significant differences found in the analysed parameters were already evident at the lowest concentrations tested, whereas in the green alga, significant differences were mostly observed only at the highest concentrations tested.

Among the analysed parameters, F_0, F_s, Rdf and NPQ were sensitive indicators of PSII damage in both organisms while F_m, ΦPSII, ETR and qP were particularly sensitive indicators in the cyanobacterium. These differences imply that the photosynthetic apparatus of the cyanobacterium is in general more sensitive to nanoceria toxicity than that of the green alga. The toxicity results obtained for both organisms overall suggest that the observed inhibition of photosynthesis by nanoceria is due to a significant impact on primary photochemical processes of PSII. The decrease in qP and increase in F_s indicate PSII reaction centre closures/inactivity, most probably due to damaged centres. This is reflected in the inhibition of the linear electron transport rate, indicating that the electron transport chain is probably blocked to some extent at the donor side of PSII (beyond Q_A), which also implies a lower capacity of PSI to drain electrons. The decrease in intrinsic PSII efficiency, which seems to be caused by the decrease in NPQ (drastically inhibited in the green alga at high nanoceria concentrations) as well as the increase in F_0, may also indicate damage to the antennae systems.

DCF fluorescence is a well known marker of cellular oxidative stress and it can detect intracellular ROS such as hydrogen peroxide, hydroxyl radicals and peroxyl radicals (Gomes et al., 2005). ROS have been reported to affect lipids, proteins and nucleic acids, leading eventually to cell death (He and Hader, 2002, Xie et al., 2009). In this respect, the presence of highly damaged or lysed cells (this report and Rodea-Palomares et al. (2011)) may be the result of loss of membrane integrity due to lipid peroxidation, which was found to occur both in the alga and in the cyanobacterium as evidenced by the BODIPY fluorescence indicator (Gomes et al., 2005). The oxidative stress generated by nanoceria in both photosynthetic organisms, even at low concentrations, may be responsible for the observed photosynthetic inhibition since the effect of increased ROS on photosynthesis performance is well documented and has been found to damage photosystem II by inhibiting the repair cycle involving the D1 protein (Latifi et al., 2009, Nishiyama et al., 2001). However, it should be pointed out that there is a fundamental difference between the cyanobacterium and the green alga in the location of the photosynthetic apparatus, which may have important implications for the way that the photosynthetic machinery of both organisms is affected by oxidative damage induced by ROS: whereas in the cyanobacterium, the photosynthetic membranes are exposed to the cytoplasm and may be directly affected by the generated ROS, in the green alga, photosynthetic complexes reside in the chloroplast and ROS may be buffered by cytoplasmic redox buffers such as glutathione (Shao et al., 2008), which might decrease further oxidative damage to the photosynthetic membranes.

How do nanoceria induce an oxidative stress which impairs photosynthesis, causes lipid peroxidation and eventually leads to cell lysis and death? Although it has been suggested that nanoceria act as radical scavenger and behave as antioxidants and have a protective effect in certain cellular systems (Chen et al., 2006, Schubert et al., 2006, Xia et al., 2008, Zhou et al., 2011), many other authors have found deleterious effects of nanoceria exposure (Kim et al., 2010, Lin et al., 2006, Park et al., 2008, Thill et al., 2006, Yokel et al., 2009, Zeyons et al., 2009, Zhang et al., 2011). There is at least a report in the literature of photocatalytic production of hydroxyl radicals and peroxidation of a model plant fatty acid by nanoceria (Rogers et al., 2010). Furthermore, Heckert et al. (2008) found that free Ce(III) is capable to redox-cycling with hydrogen peroxide to generate damaging ROS such as hydroxyl radicals and even superoxide anion radicals: they proposed that the reactivity of surface associated Ce(III) sites is the most likely source of ROS in the cellular systems where a deleterious effect of nanoceria has been observed.

DOI: 10.1016/j.aquatox.2012.06.005

Oxygenic photosynthesis is a source of ROS such as hydrogen peroxide (Asada, 1999, Asada and Baker, 2004) which may react with the Ce(III) sites at the surface of the cerium nanoparticles in close contact with the algal and particularly cyanobacterial cells (where we could observe nanoparticles attached to the cell surface and thylakoids (Rodea-Palomares et al., 2011)), and undergo an oxidative reaction which may produce hydroxyl radicals or even superoxide anions that can profoundly affect the photosynthetic machinery and impair membrane integrity by lipid peroxidation. In addition, Xia et al. (2008) found that nanoceria may also generate hydrogen peroxide under abiotic conditions. In the observed cell-nanoparticle aggregates, especially in the case of the green alga, the abiotically generated hydrogen peroxide, which readily passes through membranes, might add to that produced in the photosynthetic process, increasing the substrate amount for the oxidative reaction. Also, as pointed out by Rogers et al. (2010), the hydroxy radicals produced photocatalytically by nanoceria are of utmost importance in photosynthetic organisms since light is a requirement and light exposure also seems to be required to promote the toxic effect of nanoceria.

5. Conclusions

This study showed that nanoceria had a significant impact on the primary photochemical processes of photosystem II in the two aquatic organisms tested. ROS generation greatly increased as a result of nanoceria exposure. It is proposed that nanoceria increase the production of hydrogen peroxide (a normal ROS by-product of light-driven photosynthesis) in both the green alga and the cyanobacterium. ROS cause lipid peroxidation, compromising membrane integrity and also seriously impairing photosynthetic performance, eventually leading to cell death.

Acknowledgements

This study was supported by the Community of Madrid [grants S-0505/AMB/0321 and S-2009/AMB/1511 (Microambiente-CM)] and by the Spanish Ministry of Science and Innovation [grant CGL2010-15675, sub-programme BOS]. Ismael Rodea-Palomares is the recipient of a Ph.D. research contract from the Community of Madrid and Javier Santiago-Morales thanks the Spanish Ministry of Education for the award of an FPU grant. The authors wish to thank the Flow Cytometry and Confocal Microscopy services from the SIDI of the Universidad Autónoma de Madrid for their excellent technical assistance.

References

Allen, M.B., Arnon, D.I., 1955. Studies on nitrogen-fixing blue green algae. I Growth and nitrogen fixation by Anabaena cylindrica Lemm. PLant Physiol. 30, 366-372.

Apel, K., Hirt, H., 2004. Reactive oxygen species: metabolism, oxidative stress, and signal transduction. Annu. Rev. Plant Biol. 55, 373-399.

Armond, P.A., Björkman, O., Staehelin, L.A., 1980. Dissociation of supramolecular complexes in chloroplast membranes A manifestation of heat damage to the photosynthetic apparatus. Biochim. Biophys. Acta, Biomembr. 601, 433-442.

Asada, K., 1999. The Water-Water cycle in Chloroplasts: Scavenging of Active Oxygens and Dissipation of Excess Photons. Annu. Rev. Plant Physiol. Plant Mol. Biol. 50, 601-639.

Asada, K., Baker, N.R., 2004. Radical Production and Scavenging in the Chloroplasts Photosynthesis and the Environment. Springer Netherlands, pp. 123-150.

Björkman, O., Demmig, B., 1987. Photon yield of O2 evolution and chlorophyll fluorescence characteristics at 77 K among vascular plants of diverse origins. Planta 170, 489-504.

Calabrese, E.J., 2008. Hormesis: Why it is important to toxicology and toxicologists. Environ. Toxicol. Chem. 27, 1451-1474.

Campbell, D., Hurry, V., Clarke, A.K., Gustafsson, P., Oquist, G., 1998. Chlorophyll fluorescence analysis of cyanobacterial photosynthesis and acclimation. Microbiol. Mol. Biol. Rev. 62, 667-683.

Celardo, I., Pedersen, J.Z., Traversa, E., Ghibelli, L., 2011. Pharmacological potential of cerium oxide nanoparticles. Nanoscale 3, 1411-1420.

Chen, J., Patil, S., Seal, S., McGinnis, J.F., 2006. Rare earth nanoparticles prevent retinal degeneration induced by intracellular peroxides. Nat. Nanotechnol. 1, 142-150.

Das, M., Patil, S., Bhargava, N., Kang, J.-F., Riedel, L.M., Seal, S., Hickman, J.J., 2007. Auto-catalytic ceria nanoparticles offer neuroprotection to adult rat spinal cord neurons. Biomaterials 28, 1918-1925.

Deblois, C.P., Juneau, P., 2010. Relationship between photosynthetic processes and microcystin in Microcystis aeruginosa grown under different photon irradiances. Harmful Algae 9, 18-24.

Fai, P.B., Grant, A., Reid, B., 2007. Chlorophyll a fluorescence as a biomarker for rapid toxicity assessment. Environ. Toxicol. Chem. 26, 1520-1531.

Fracheboud, Y., Jompuk, C., Ribaut, J.M., Stamp, P., Leipner, J., 2004. Genetic analysis of cold-

tolerance of photosynthesis in maize. Plant Mol. Biol. 56, 241-253.
Genty, B., Briantais, J.-M., Baker, N.R., 1989. The relationship between the quantum yield of photosynthetic electron transport and quenching of chlorophyll fluorescence. Biochim. Biophys. Acta Gen. Subj. 990, 87-92.
Geoffroy, L., Dewez, D., Vernet, G., Popovic, R., 2003. Oxyfluorfen toxic effect on S. obliquus evaluated by different photosynthetic and enzymatic biomarkers. Arch. Environ. Contam. Toxicol. 45, 445-452.
Geoffroy, L., Gilbin, R., Simon, O., Floriani, M., Adam, C., Pradines, C., Cournac, L., Garnier-Laplace, J., 2007. Effect of selenate on growth and photosynthesis of *Chlamydomonas reinhardtii*. Aquat. Toxicol. 83, 149-158.
Giráldez-Ruiz, N., Mateo, P., Bonilla, I., Fernández-Piñas, F., 1997. The relationship between intracellular pH, growth characteristics and calcium in the cyanobacterium Anabaena sp. strain PCC7120 exposed to low pH. New Phytol. 137, 599-605.
Gomes, A., Fernandes, E., Lima, J.L.F.C., 2005. Fluorescence probes used for detection of reactive oxygen species. J. Biochem. Bioph. Methods 65, 45-80.
Havaux, M., 1993. Characterization of thermal damage to the photosynthetic electron transport system in potato leaves. Plant Sci. 94, 19-33.
He, Y.-Y., Hader, D.-P., 2002. Reactive oxygen species and UV-B: effect on cyanobacteria. Photochem. Photobiol. Sci. 1, 729-736.
Heckert, E.G., Seal, S., Self, W.T., 2008. Fenton-like reaction catalyzed by the rare earth inner transition metal cerium. Environ. Sci. Technol. 42, 5014-5019.
Kim, I.S., Baek, M., Choi, S.J., 2010. Comparative cytotoxicity of Al_2O_3, CeO_2, TiO_2 and ZnO nanoparticles to human lung cells. J. Nanosci. Nanotechnol. 10, 3453-3458.
Korsvik, C., Patil, S., Seal, S., Self, W.T., 2007. Superoxide dismutase mimetic properties exhibited by vacancy engineered ceria nanoparticles. Chem. Commun. 1056-1058.
Krause, G.H., Weis, E., 1991. Chlorophyll Fluorescence and Photosynthesis: The Basics. Annu. Rev. Plant Physiol. Plant Mol. Biol. 42, 313-349.
Kummerová, M., Barták, M., Dubová, J., Tříska, J., Zubrová, E., Zezulka, Š., 2006. Inhibitory Effect of Fluoranthene on Photosynthetic Processes in Lichens Detected by Chlorophyll Fluorescence. Ecotoxicology 15, 121-131.
Latifi, A., Ruiz, M., Zhang, C.C., 2009. Oxidative stress in cyanobacteria. FEMS Microbiol. Rev. 33, 258-278.
Liang, C., Zhang, G., Zhou, Q., 2011. Effect of cerium on photosynthetic pigments and photochemical reaction activity in soybean seedling under ultraviolet-B radiation stress. Biol. Trace Elem. Res. 142, 796-806.
Lin, W., Huang, Y.W., Zhou, X.D., Ma, Y., 2006. Toxicity of cerium oxide nanoparticles in human lung cancer cells. Int. J. Toxicol. 25, 451-457.
Marker, A.F.H., 1972. The use of acetone and methanol in the estimation of chlorophyll in the presence of phaeophytin. Freshwater Biol. 2, 361-385.
Maxwell, K., Johnson, G.N., 2000. Chlorophyll fluorescence-A practical guide. J. Exp. Bot. 51, 659-668.
Navarro, E., Baun, A., Behra, R., Hartmann, N.B., Filser, J., Miao, A.J., Quigg, A., Santschi, P.H., Sigg, L., 2008. Environmental behavior and ecotoxicity of engineered nanoparticles to algae, plants, and fungi. Ecotoxicology 17, 372-386.
Nishiyama, Y., Yamamoto, H., Allakhverdiev, S.I., Inaba, M., Yokota, A., Murata, N., 2001. Oxidative stress inhibits the repair of photodamage to the photosynthetic machinery. EMBO J. 20, 5587-5594.
Pan, X., Deng, C., Zhang, D., Wang, J., Mu, G., Chen, Y., 2008. Toxic effects of amoxicillin on the photosystem II of *Synechocystis* sp. characterized by a variety of in vivo chlorophyll fluorescence tests. Aquat. Toxicol. 89, 207-213.
Papageorgiou, G.C., Tsimilli-Michael, M., Stamatakis, K., 2007. The fast and slow kinetics of chlorophyll a fluorescence induction in plants, algae and cyanobacteria: a viewpoint. Photosynth. Res. 94, 275-290.
Park, E.-J., Choi, J., Park, Y.-K., Park, K., 2008. Oxidative stress induced by cerium oxide nanoparticles in cultured BEAS-2B cells. Toxicology 245, 90-100.
Porra, R.J., Thompson, W.A., Kriedemann, P.E., 1989. Determination of accurate extinction coefficients and simultaneous equations for assaying chlorophylls a and b extracted with four different solvents: verification of the concentration of chlorophyll standards by atomic absorption spectroscopy. Biochim. Biophys. Acta Bioenergetics 975, 384-394.
Ricart, M., Guasch, H., Alberch, M., Barcelo, D., Bonnineau, C., Geiszinger, A., Farre, M., Ferrer, J., Ricciardi, F., Romani, A.M., Morin, S., Proia, L., Sala, L., Sureda, D., Sabater, S., 2010. Triclosan persistence through wastewater treatment plants and its potential toxic effects on river biofilms. Aquat. Toxicol. 100, 346-353.
Rodea-Palomares, I., Boltes, K., Fernández-Piñas, F., Leganés, F., Garcia-Calvo, E., Santiago, J., Rosal, R., 2011. Physicochemical characterization and ecotoxicological assessment of CeO_2 nanoparticles using two aquatic microorganisms. Toxicol. Sci. 119, 135-145.

DOI: 10.1016/j.aquatox.2012.06.005

Rogers, N.J., Franklin, N.M., Apte, S.C., Batley, G.E., Angel, B.M., Lead, J.R., Baalousha, M., 2010. Physico-chemical behaviour and algal toxicity of nanoparticulate CeO_2 in freshwater. J Environ. Chem. 7, 10.

Roháček, K., 2002. Chlorophyll Fluorescence Parameters: The Definitions, Photosynthetic Meaning, and Mutual Relationships. Photosynthetica 40, 13-29.

Schubert, D., Dargusch, R., Raitano, J., Chan, S.-W., 2006. Cerium and yttrium oxide nanoparticles are neuroprotective. Biochem. Biophys. Res. Commun. 342, 86-91.

Shao, H.B., Chu, L.Y., Lu, Z.H., Kang, C.M., 2008. Primary antioxidant free radical scavenging and redox signaling pathways in higher plant cells. Int. J. Biol. Sci. 4, 8-14.

Thill, A., Zeyons, O., Spalla, O., Chauvat, F., Rose, J., Auffan, M., Flank, A.M., 2006. Cytotoxicity of CeO_2 nanoparticles for *Escherichia coli*. Physico-chemical insight of the cytotoxicity mechanism. Environ. Sci. Technol. 40, 6151-6156.

Tiede, K., Hassell, M., Breitbarth, E., Chaudhry, Q., Boxall, A.B.A., 2009. Considerations for environmental fate and ecotoxicity testing to support environmental risk assessments for engineered nanoparticles. J. Chromatogr. A 1216, 503-509.

Toth, S.Z., Schansker, G., Strasser, R.J., 2005. In intact leaves, the maximum fluorescence level (FM) is independent of the redox state of the plastoquinone pool: A DCMU-inhibition study. Biochim. Biophys. Acta Bioenergetics 1708, 275-282.

Xia, T., Kovochich, M., Liong, M., Madler, L., Gilbert, B., Shi, H., Yeh, J.I., Zink, J.I., Nel, A.E., 2008. Comparison of the mechanism of toxicity of zinc oxide and cerium oxide nanoparticles based on dissolution and oxidative stress properties. ACS Nano 2, 2121-2134.

Xie, Z., Wang, Y., Liu, Y., Liu, Y., 2009. Ultraviolet-B exposure induces photo-oxidative damage and subsequent repair strategies in a desert cyanobacterium *Microcoleus vaginatus* Gom. Eur. J. Soil Biol. 45, 377-382.

Yokel, R.A., Florence, R.L., Unrine, J.M., Tseng, M.T., Graham, U.M., Wu, P., Grulke, E.A., Sultana, R., Hardas, S.S., Butterfield, D.A., 2009. Biodistribution and oxidative stress effects of a systemically-introduced commercial ceria engineered nanomaterial. Nanotoxicology 3, 234-248.

Yuguan, Z., Min, Z., Luyang, L., Zhe, J., Chao, L., Sitao, Y., Yanmei, D., Na, L., Fashui, H., 2009. Effects of cerium on key enzymes of carbon assimilation of spinach under magnesium deficiency. Biol. Trace Elem. Res. 131, 154-164.

Zeyons, O., Thill, A., Chauvat, F., Menguy, N., Cassier-Chauvat, C., Oréar, C., Daraspe, J., Auffan, M., Rose, J., Spalla, O., 2009. Direct and indirect CeO_2 nanoparticles toxicity for *Escherichia coli* and *Synechocystis*. Nanotoxicology 3, 284-295.

Zhang, H., He, X., Zhang, Z., Zhang, P., Li, Y., Ma, Y., Kuang, Y., Zhao, Y., Chai, Z., 2011. Nano-CeO_2 exhibits adverse effects at environmental relevant concentrations. Environ. Sci. Technol. 45, 3725-3730.

Zhou, X., Wong, L.L., Karakoti, A.S., Seal, S., McGinnis, J.F., 2011. Nanoceria inhibit the development and promote the regression of pathologic retinal neovascularization in the Vldlr knockout mouse. PLoS One 6, e16733.

Zhu, B., Yang, X.T., Xu, J., Zhu, Z.G., Ji, S.J., Sun, M.T., Sun, J.C., 2003. Innovative low temperature SOFCs and advanced materials. J Power Sources 118, 47-53.

DOI: 10.1016/j.aquatox.2012.06.005

Supplementary Material

An insight into the mechanisms of nanoceria toxicity in aquatic photosynthetic organisms

Ismael Rodea-Palomares[1], Soledad Gonzalo[2], Javier Santiago-Morales[2], Francisco Leganés[1], Eloy García-Calvo[2,3], Roberto Rosal[2], Francisca Fernández-Piñas[1]

Ismael Rodea-Palomares[1], Francisco Leganés[1], Roberto Rosal[2], Francisca Fernández-Piñas[1,*]

[1] Departamento de Biología, Facultad de Ciencias, Universidad Autónoma de Madrid, Cantoblanco, E-28049 Madrid, Spain
[2] Departamento de Ingeniería Química, Universidad de Alcalá, Alcalá de Henares, E-28871 Madrid, Spain
[3] Advanced Study Institute of Madrid, IMDEA-Agua, Parque Científico Tecnológico, E-28805, Alcalá de Henares, Madrid, Spain

Table S1. Composition of AA/8 + N medium (Allen & Arnon modified medium) as final concentrations of its components.

Component	µM	Component	µM	Component	µM
$MgSO_4$	0.13	KNO_3	6.25	$ZnSO_4$	0.10
$CaCl_2$	0.06	Na_2EDTA	9.59	$CuSO_4$	0.04
NaCl	0.50	$FeSO_4$	8.65	H_3BO_3	5.78
K_2HPO_4	0.25	$MnCl_2$	1.14	NH_4VO_3	0.02
$NaNO_3$	6.25	MoO_3	0.16	$CoCl_2$	0.02

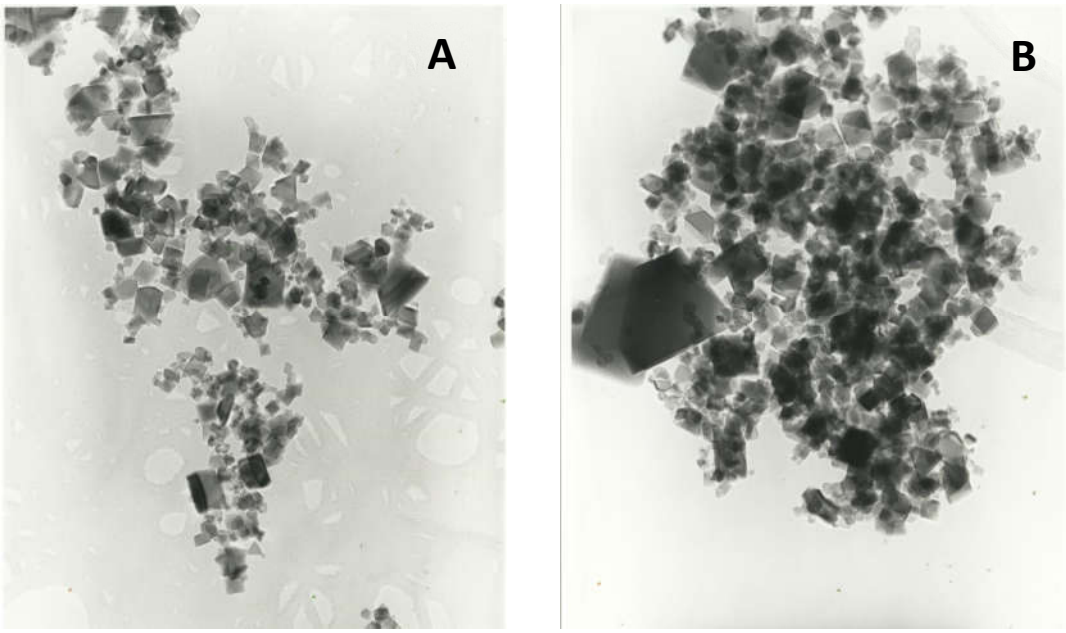

Figure S1. TEM micrographs of suspensions of N50 particles in algal medium (A) and cyanobacterial medium (B) at 100 mg/L.

DOI: 10.1016/j.aquatox.2012.06.005